Journal of Solid State Chemistry 183 (2010) 2650–2655

Contents lists available at ScienceDirect

Journal of Solid State Chemistry

journal homepage: www.elsevier.com/locate/jssc

Crystal structure and magnetic properties of $Na_2Ni^{II}(HPO_3)_2$

Wassim Maalej [a,b,*], Serge Vilminot [a,**], Zakaria Elaoud [b], Tahar Mhiri [b], Mohamedally Kurmoo [c]

[a] Département de Chimie des Matériaux Inorganiques, IPCMS, UMR CNRS-UdS 7504, 23 rue du Loess, BP 43, 67034 Strasbourg Cedex 2, France
[b] Laboratoire de l'Etat Solide, Département de Chimie, Faculté des Sciences de Sfax, BP 802, Route de Soukra, 3018 Sfax, Tunisia
[c] Laboratoire DECOMET, CNRS-UMR 7177, Université de Strasbourg, 4 rue Blaise Pascal, 67000 Strasbourg Cedex 1, France

ARTICLE INFO

Article history:
Received 16 July 2010
Received in revised form
1 September 2010
Accepted 6 September 2010
Available online 15 September 2010

Keywords:
Inorganic framework
Hydrothermal synthesis
Triangular chain
Antiferromagnet

ABSTRACT

$Na_2Ni(HPO_3)_2$, obtained as light yellow-green crystals under mild hydrothermal conditions, crystallizes in the orthorhombic *Pnma* space-group with lattice parameters: $a=11.9886(3)$, $b=5.3671(2)$, $c=9.0764(3)$ Å, $V=584.01$ Å^3, $Z=4$. The structure consists of zig-zag chains of NiO_6 octahedra bridged by two HPO_3^{2-} and the chains are further connected through HPO_3^{2-} to four nearest chains to form a three dimensional framework, delimiting intersecting tunnels in which the sodium ions are located. The Na cations reside in the irregular $Na(1)O_5$, Na–O of 2.276–2.745 Å, and $Na(2)O_9$, Na–O of 2.342–2.376 Å, environments. The presence of the phosphite monoanion has been further confirmed by IR spectroscopy. Due to the 3D framework of Ni connected by O–P–O bridges, the magnetic susceptibility behaves as a paramagnet above 100 K ($C=1.49(2)$ emu K mol^{-1}, $\mu_{eff}=3.45$ μ_B, $\Theta=-39(2)$ K) and below 6 K, it orders antiferromagnetically as confirmed the sharp drop and the non-Brillouin behavior of the isothermal magnetization at 2 K.

1. Introduction

Considerable efforts are being devoted to the development of functional materials with electrical, magnetic and optical properties for applications [1]. For magnetic materials certain criteria have to be met in order to establish long range magnetic ordering [2]. Among the most important factor for a chemist designing magnets is the chemical connection between the metals carrying the moment as the Curie temperature decreases rapidly with increasing number of atoms in the chemical bridge [3]. The second important factor is the dimensionality of the network, as the Curie temperature has the same tendency with reducing dimensionality. So, there is a great interest to create materials with small bridges while trying to retain a 3D structure. Consequently, coordination polymers of paramagnetic transition metals have been of interest for a number of years. More recently, there is considerable interest by magneto-chemists in using three-atom bridges due to the wider range of chemicals available and only few systems are known where three-atom connectors bridge all pairs uniformly. Amongst them are those containing azide [4], imidazole [5], dicyanamide [6], carbonate [7], oxalate [8] and formate [9]. The latter has been of much importance to us in the development of materials exhibiting dual property, such as porosity and magnetism [3,9]. Following this line of work, we are searching for other ligands to mimic the formate ion and our first choice was hypophosphite, $H_2PO_2^-$, complexes of transition metals but this has not been successful so far and resulted in only chain compounds [10]. Here, we present the accidental isolation of a 3D framework consisting of Ni and HPO_3^{2-} connections which orders as an antiferromagnet at 6 K. It is interesting to note that the bridging unit is the doubly charged HPO_3^{2-} that is derived from phosphorous acid (H_3PO_3). It frequently forms transition metal complexes with the singly charged $H_2PO_3^-$. Furthermore, only a few mixed-metal phosphites containing sodium and a transition metal have been reported, for example: $NaCo(H_2PO_3)_3\cdot H_2O$ [11], $NaMn(H_2PO_3)_3\cdot H_2O$ [12], $NaZn(H_2PO_3)_3\cdot H_2O$ [13], $Na_2[Fe(HPO_3)_2]$ [14], $Na_2[Co(HPO_3)_2]$ [14], $Na_2Zn_3(HPO_3)_4$ [15], and $NaMg(H_2PO_3)_3\cdot H_2O$ [16]. In this paper, we present the hydrothermal synthesis, crystal structure determination and infrared spectral and magnetic properties of $Na_2Ni(HPO_3)_2$.

2. Experimental

2.1. Synthesis

$Na_2Ni(HPO_3)_2$ was synthesized under mild hydrothermal conditions starting from $NiCl_2\cdot 6H_2O$ (2 mmol), H_3PO_3 (32 mmol), *L*-phenylalanine ($C_6H_5CH_2CH(NH_2)CO_2H$) (2 mmol) and NaOH (30 mmol). The mixture of these constituents in a volume of

* Corresponding author at: Département de Chimie des Matériaux Inorganiques, IPCMS, UMR CNRS-UdS 7504, 23 rue du Loess, BP 43, 67034 Strasbourg Cedex 2, France. Fax: +33 3 88 10 72 47.
** Corresponding author. Fax: +33 3 88 10 72 47.
E-mail addresses: maalej_wassim@yahoo.fr (W. Maalej), vilminot@ipcms.u-strasbg.fr (S. Vilminot).

0022-4596/$ - see front matter © 2010 Elsevier Inc. All rights reserved.
doi:10.1016/j.jssc.2010.09.010

5 mL of water and 20 mL of methanol was stirred to homogeneity. After that, it was poured into a PTFE-lined stainless steel pressure vessel (fill factor 75%) and heated at 150 °C for 5 days, followed by slow cooling to room temperature. The resultant yellow green crystals with a small amount of a green powder were retrieved by filtration, washed with methanol and acetone, finally dried at room temperature. The initial pH of the reaction mixture was approximately 3.5. The crystals were manually separated and washed before use for other measurements.

2.2. Crystal structure determination

A crystal with a pyramidal habit was mounted on a glass fiber and placed on the Nonius Kappa CCD diffractometer using Mo$K\alpha$ radiation (λ=0.71073 Å) for data collection (173 K, 7126 total reflections, 920 unique observed reflections, R_{int}=0.0244). The crystal structure has been solved from a three-dimensional Patterson function allowing nickel, phosphorus and sodium atoms initially to be found. The positions of oxygen and hydrogen atoms were obtained from difference Fourier maps. The final refinement using anisotropic temperature factors for all atoms but hydrogen and 889 independent reflections with $F_0 > 2\sigma$ (F_0), yields R=0.0186 and R_w=0.0486. All calculations were performed using the programs SHELXS 97 and SHELXL 97 [17]. Experimental conditions and crystal data for single-crystal diffraction data collection are reported in Table 1, fractional atomic coordinates in Table 2 and selected interatomic distances and angles in Table 3.

2.3. Physicochemical characterization techniques

Infrared spectra were recorded using a Digilab Excalibur Series FTIR spectrometer by transmission through KBr pellets containing 1% of the crystals. Powder X-ray diffraction patterns were recorded using a D8 Bruker diffractometer (Cu$K\alpha_1$ 1.5406 Å), equipped with a front monochromator. Magnetization measurements were performed in the range 2–300 K and ±50 kOe by means of a Quantum Design MPMS-XL SQUID magnetometer.

3. Results and discussion

3.1. Synthesis

The yellow-green crystals were found to be without the starting organic material, *L*-phenylalanine and a single crystal X-ray analysis reveals it to be $Na_2Ni(HPO_3)_2$. X-ray powder diffraction identified the green powder as $Ni(H_2O)_2$(*L*-phenylalanine)$_2$ whose structure from single crystal diffraction will be reported elsewhere. Our synthetic route which resulted in the nickel phosphite compound is therefore very different from the one reported by Liu et al. [14] for the corresponding iron and cobalt analogues. They started from $MCl_2 \cdot 6H_2O$ (M=Fe, Co), NaOH and H_3PO_3 while ammonia was used to control the pH. These authors evidence the fact that the nature of the resulting phase is strongly pH dependent since $Na_2M(HPO_3)_2$ was obtained

Table 2
Fractional atomic coordinates and temperature factors for $Na_2Ni(HPO_3)_2$.

	x	y	z	U_{eq} or U^*_{iso} (Å^2)
Ni	0.33869(2)	0.25	0.63616(3)	0.00612(10)
P(1)	0.48199(5)	−0.25	0.62377(6)	0.00588(13)
P(2)	0.31492(5)	0.25	0.99986(6)	0.00644(13)
Na(1)	0.59438(8)	0.25	0.77733(11)	0.0120(2)
Na(2)	0.22103(8)	0.25	0.32509(10)	0.0129(2)
O(1)	0.44849(9)	−0.0168(2)	0.70973(12)	0.0098(2)
O(2)	0.26757(14)	0.25	0.84445(17)	0.0112(3)
O(3)	0.21425(10)	−0.0137(2)	0.58414(13)	0.0140(3)
O(4)	0.39618(13)	0.25	0.42205(17)	0.0099(3)
H(1)	0.435(2)	0.25	0.996(3)	0.002*
H(2)	0.421(2)	−0.25	0.503 (3)	0.002(6)*

* U_{iso} for hydrogen atoms and not refined for H(1).

Table 3
Selected bond lengths (Å) and angles (deg.) for $Na_2Ni(HPO_3)_2$.

Atoms	Distance (Å)	Atoms	Angle (deg.)
Ni–O1	2.0566(11)	O1–Ni–O1^{i}	88.27(7)
Ni–O2	2.0739(16)	O1–Ni–O4	95.28(5)
Ni–O4	2.0619(15)	O1–Ni–O2	88.12(5)
Ni–O3	2.1099(12)	O1–Ni–O3	93.33(5)
P1–O1	1.5284(12)	O1–Ni–O3^{i}	172.90(5)
P1–O4	1.5186(16)	O4–Ni–O2	175.25(7)
P1–H2	1.32(3)	O4–Ni–O3	91.46(5)
P2–O2	1.5205(17)	O2–Ni–O3	85.03(5)
P2–O3	1.5218(12)	O3–Ni–O3^{i}	84.26(7)
P2–H1	1.44(3)	O4–P1–O1	113.11(6)
Na1–O1	2.3424(14)	O1–P1–O1^{iii}	109.92(9)
Na1–O2	2.3522(19)	O2–P2–O3^{iv}	112.37(6)
Na1–O3	2.3768(14)	O3–P2–O3^{v}	112.89(10)
Na2–O1	2.6062(14)	O4–P1–H2	107.8(11)
Na2–O2	2.6928(19)	O1–P1–H2	106.2(6)
Na2–O3	2.7456(15)	O2–P2–H1	110.5(10)
Na2–O3	2.6444(15)	O3–P2–H1	104.0(5)
Na2–O4	2.2767(18)		

Table 1
Details of X-ray diffraction data collection and refinement results for $Na_2Ni(HPO_3)_2$.

Compound	$Na_2Ni(HPO_3)_2$	Radiation	Mo$K\alpha$ (λ=0.71073 Å)
Color/shape	Yellow-green/pyramidal	Crystal dimensions (mm)	0.35 × 0.26 × 0.17
Molecular weight (g mol^{-1})	264.6	Reflections collected	7126
Space group	*Pnma*	Independent reflections	920
Temperature (K)	173	Reflections with $I > 2\sigma$ (I)	889
a (Å)	11.9886(3)	Range of h, k, l	−15/16, −7/7, −12/12
b (Å)	5.3671(2)	F(000)	520
c (Å)	9.0764(3	GOF	1.004
Volume (Å^3)	584.01	$R1$ [a]	0.0185
Z	4	R_w [b]	0.0487
D_{meas}, D_{calc} (Mg m^{-3})	2.98, 3.01	$\Delta\rho$(max)/$\Delta\rho$(min)	0.598/−0.449 e Å^{-3}
μ (mm^{-1})	3.985	Absorption correction	Multiscan with Sadabs T_{min} 0.4743, T_{max} 0.5340

[a] $R1 = \Sigma||F_o|-|F_c||/\Sigma|F_o|$.
[b] $w = 1/[\sigma^2(F_o^2)+(0.0259P)^2+0.86P]$ with $P=(F_o^2+2F_c^2)/3$.

only for pH > 5. In our case, the measured pH value was 3.5 but as the solvent is a mixture of water and methanol, the pH value is not comparable. We believe the presence of methanol increases the pressure inside the reactor and favors crystal growth.

3.2. Crystal structure

The key feature of the structure of $Na_2Ni(HPO_3)_2$ is the three dimensional framework of nickel connected through O–P–O bridges of HPO_3. This is an interesting structure which is isostructural to the iron and cobalt analogues and may be compared to NaCl frameworks observed for $AM^{II}(HCOO)_3$ [9] and $V(H_2PO_2)_3$ [18]. The unit cell of $Na_2Ni(HPO_3)_2$ consists of one nickel, two different HPO_3 and two independent Na. The nickel adopts a distorted octahedral coordination with six oxygen atoms from six independent HPO_3. While four of the HPO_3 are involved in the construction of zig-zag chains along the *b*-axis, the other two are involved in joining these chains to form the 3D framework with hexagonal patterned channels. The Na atoms fill the cavities created within the framework and are bonded to the oxygen atoms (Fig. 1).

The octahedron of NiO_6 can be considered as Jahn–Teller distorted with two long and four short Ni–O bonds; the mean Ni–O bond distance is 2.08 Å. The *cis*- and *trans*-O–Ni–O angles range from 84.26(7)° to 95.28(5)° and from 172.90(5)° to 175.25(6)°, respectively. These values are typical for Ni in an octahedral oxygen environment. The HPO_3 adopts a flattened tetrahedral geometry with P–O bond lengths in the range of 1.519(2)–1.528(1) Å for HP(1)O3 and 1.520(2)–1.521(1) Å for HP(2)O3 and the P–H mean distance of 1.38(3) Å with P(1)–H(2)=1.32(3) Å and P(2)–H(1)=1.44(3) Å. As observed from the X-ray analysis the P–H lengths appear to be different but are within the expected ranges [14,18]. The hydrogen atoms are quite far from the neighboring oxygen atoms (≥ 2.68 Å) for any hydrogen bond to be considered.

The Na(1) atom, residing in a roughly distorted square pyramid, connects HPO_3 and NiO_6. Na(1) is coordinated to 5 oxygen atoms with Na–O bond lengths in the range of 2.342(1)–2.377(1) Å. The mean Na–O distance, 2.358 Å, agrees with the sum of ionic radii for 5-fold coordination, 2.36 Å. Na(2) are coordinated to nine oxygen atoms and build ribbons of NaO_9 polyhedra by sharing two corners, with Na–O distances ranging from 2.277(2) to 2.746(2) Å (Fig. 2). The NaO_9 polyhedra are strongly distorted and form infinite ribbons and chains as viewed along the crystallographic *b* and *c* directions, respectively, with Na–Na distance of 5.318 Å. Whereas the mean Na–O distance from the 8 longest bonds, 2.67 Å, is very close to the sum of the ionic radii, 2.68 Å, the last Na–O distance is very short, 2.277(2) Å. Therefore, it can be considered that Na^+ defines a privileged bond with one oxygen atom of the channel and the corresponding Na–O bond presents a much more covalent character than the interaction of Na^+ with the other O^{2-} ions in its neighborhood. The O–Na(1)–O and O–Na(2)–O angles are close to those found in the literature

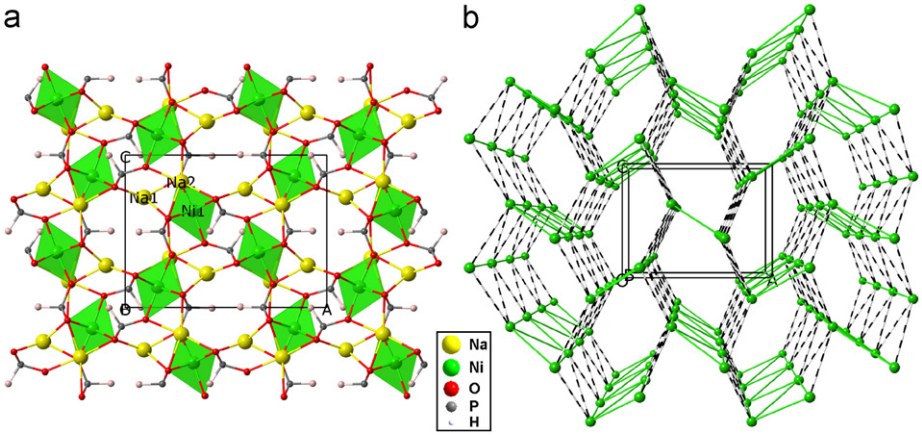

Fig. 1. (a) Projection of the structure on the *ac* plane and (b) the 3D-network of nickel atoms, the dashed lines connect the diamond chains of nickel.

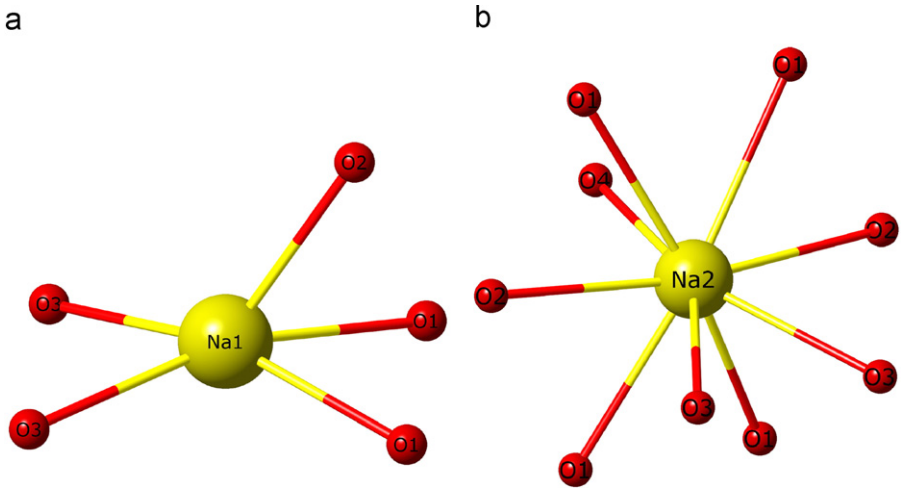

Fig. 2. Coordination environments of (a) Na1 and (b) Na2.

for the similar structures [14,19,20]. Na(1) sits in the 12-member ring channels and Na(2) in the six-member rings.

Within the chains the Ni…Ni distances are 5.317 and 5.367 Å, thus generating an isosceles triangular chain (Fig. 3a). The chains are connected to one another via the HPO_3 bridges with Ni…Ni distances of 5.685 Å. Each nickel center has eight nickel neighbors (Fig. 3b), four along the zig-zag chain and two pairs belonging to adjacent chains. The $Na_2Ni(HPO_3)_2$ is isostructural with the recently reported $M_2Ni(HPO_3)_2$ (M=Fe and Co) compounds (Table 4) [14] and the unit cell parameters vary with the cationic radius of the transitional metal, viz: Fe > Co > Ni.

3.3. X-ray powder diffraction

The X-ray powder diffraction pattern (Fig. 4) of selected ground crystals has been fully indexed starting from the unit cell parameters obtained from single crystal data. The parameters have been refined using the Fullprof program giving a=12.0207(5) Å, b=5.3689(2) Å, c=9.0876(4) Å, V=586.49(7) Å^3 in agreement with the data of Table 1. No other phase was detected within the detection limit of the technique. Complete analysis of the powder pattern confirms that $Na_2Ni(HPO_3)_2$ crystallizes in the orthorhombic *Pnma* system. The density was measured at room temperature by flotation in tetrachlorobenzene. The average value of density, D_m=2.98 Mg m^{-3}, yields a value of four formula units and a calculated density, D_x=3.01 Mg m^{-3}.

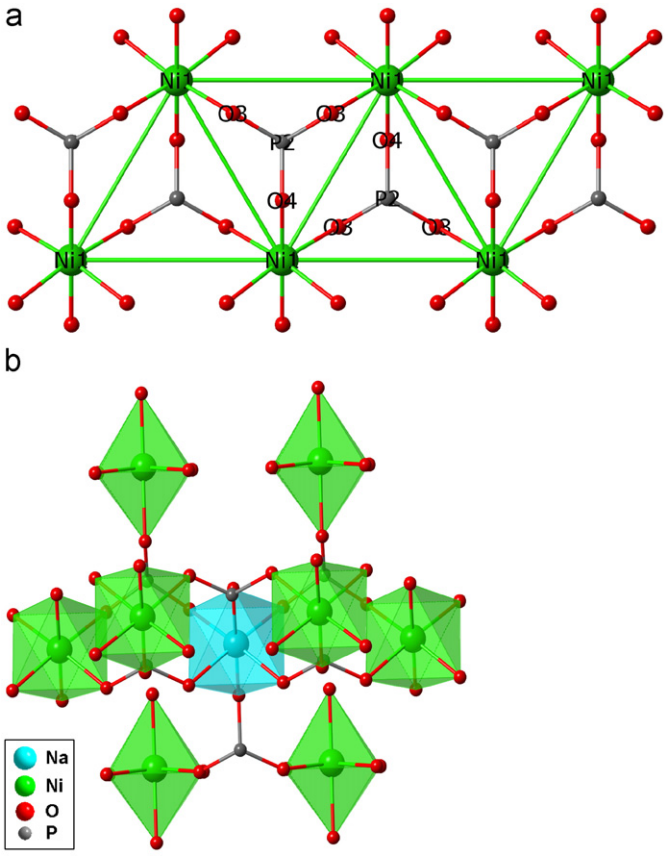

Fig. 3. (a) A diamond chain of nickel showing the connections via the HPO_3 units and (b) the near-neighbor nickel atoms around a central one and their connections.

Table 4
Unit-cell parameters of the $Na_2M(HPO_3)_2$ (M=Ni, Fe and Co) compounds, average M–O bond length and ionic radii of the metallic cations.

Compound	M=Fe	M=Co	M=Ni
a (Å)	12.169(4)	12.091(3)	11.9886(3)
b (Å)	5.441(2)	5.400(4)	5.3671(2)
c (Å)	9.164(3)	9.115(2)	9.0764(3)
V (Å^3)	606.7(4)	595.1(3)	584.01(3)
M–O	2.137	2.110	2.078
Ionic radius (Å)	0.77	0.735	0.70

3.4. Infrared spectroscopy

The IR spectrum of $Na_2Ni(HPO_3)_2$ of a powder at room temperature is illustrated in Fig. 5. The vibrational bands and their frequencies are given in Table 5. These results are similar to those found in other related compounds [21] containing the phosphite ion. According to Tsuboi [22] and Bickley et al. [23], the "free" HPO_3^{2-} ions has C_{3v} symmetry and its nine internal vibrations are divided between the following six normal modes:

$\nu_1(A_1)$=2315 cm^{-1} (νPH)
$\nu_2(E)$=1027 cm^{-1} (δPH, γPH)
$\nu_3(A_1)$=979 cm^{-1} (νPO_3)
$\nu_3(E)$=1085 cm^{-1} ($\nu_a PO_3$)
$\nu_4(A_1)$=567 cm^{-1} ($\delta_s PO_3$)
$\nu_4(E)$=465 cm^{-1} ($\delta_a PO_3$)

The strong bands observed at 470 and 500 cm^{-1} are attributed to $\delta_a(PO_3)$ and ν(Ni–O), respectively. The ν_4 ($\delta_s PO_3$) deformation modes of the HPO_3 group are supposed to appear at 584, 638 and 696 cm^{-1} according to Ref. [24]. The bands at 850 and 996 cm^{-1} are assigned to $\nu_3(\nu PO_3)$ vibrations. The bending vibrations (ν_2) of the P–H bond were found at 1028 and 1058 cm^{-1}, although these bands may also arise from the stretching vibrations of the PO_3 group whereas the stretching $\nu_1(\nu$PH) appear at 2360 and 2496 cm^{-1}.

3.5. Magnetic properties

The magnetic susceptibility of a polycrystalline sample of selected crystals is shown in Fig. 6. The behavior at high temperature (100–300 K) follows the Curie–Weiss law, $\chi = C/(T-\theta)$, with C=1.49(2) emu K/mol and $\theta = -39(2)$ K. The effective magnetic moment and Landé g factor calculated from the Curie constant are 3.45 μ_B and 2.44, respectively. These values are slightly higher than the expected ones, 2.83 μ_B and 2.29, respectively. The magnetic susceptibility reaches a maximum at 6.0 K, followed by a sharp decrease to 2 K. This peak is associated with long-range antiferromagnetic ordering which resulted in a non-Brillouin behavior and low magnetization at 2 K. The cobalt analogue orders as an antiferromagnet at 3 K and for the iron analogue no ordering was observed in the measurements in a field of 10 kOe [14].

4. Conclusion

$Na_2Ni(HPO_3)_2$ was accidently obtained under mild hydrothermal conditions. The structure consists of a three-dimensional, compact framework formed by edge sharing NiO_6 octahedra linked by O–P–O bridges of HPO_3^{2-}. The presence of two δ(PH) bands in the IR spectrum is consistent with the existence of the crystallographically independent phosphite groups in the structure. The magnetic measurements indicate a long range antiferromagnetic ordering below T_N=6 K via super–super-exchange through the phosphite anions.

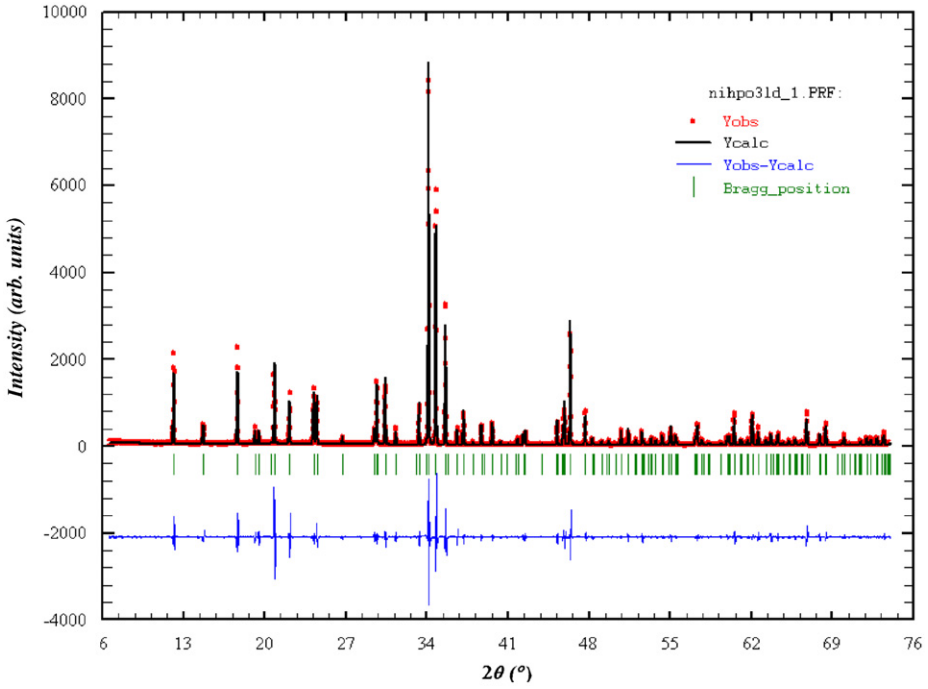

Fig. 4. Rietveld refinement of the X-ray diffraction powder pattern of $Na_2Ni(HPO_3)_2$ ($CuK\alpha_1$ radiation).

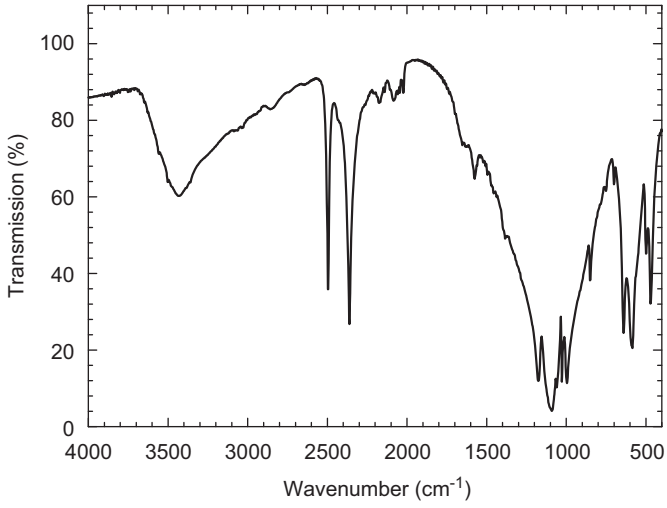

Fig. 5. Infrared spectrum of $Na_2Ni(HPO_3)_2$.

Table 5
Observed bands (values in cm^{-1}) in the IR spectrum of $Na_2Ni(HPO_3)_2$.

IR tentative assignment
2496 (s) ν(PH)
2361 (s)
1176 (s) $\nu_a PO_3$
1092 (s)
1058 (w) δPH, γPH
1028 (m)
996 (s) $\nu(PO_3)$
850 (m)
696 (w) $\delta_s(PO_3)$
638 (s)
584 (s)
499 (w) $\delta_a(PO_3)$
470 (s) ν(NiO)

ν=stretching, δ=in-plane deformation, γ=out-of-plane deformation, s=symmetric, as=asymmetric, s=strong, m=medium, w=weak.

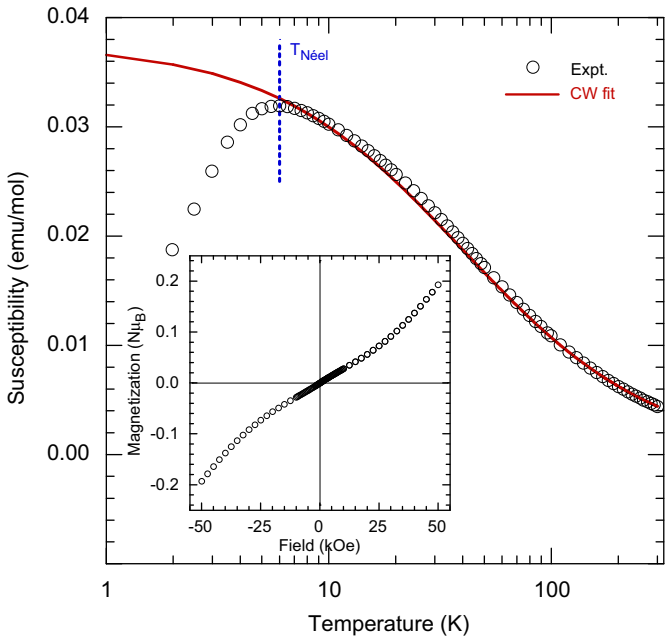

Fig. 6. Temperature dependence of the magnetic susceptibility and the isothermal magnetization at 2 K (inset) of $Na_2Ni(HPO_3)_2$.

Acknowledgment

This work was funded by the CNRS-France. We thank Natalie Kyritsakas for the X-ray data collection.

References

[1] P. Day, in: Molecules into Materials: Case Studies in Materials Chemistry—Mixed Valency, Magnetism and Superconductivity, World Scientific Publishing, Singapore, 2007.
[2] S.J. Blundell, in: Magnetism in Condensed Matter, Oxford University Press, 2001;

A. Herpin, in: Theorie du Magnétisme, Presse Universitaire de France, Paris, 1968.
[3] M. Kurmoo, Chem. Soc. Rev. 38 (2009) 1353–1379.
[4] J. Ribas, A. Escuer, M. Monfort, R. Vicente, R. Cortés, L. Lezama, T. Rojo, Coord. Chem. Rev. 193–195 (1999) 1027–1068.
[5] Y.-Q. Tian, C.-X. Cai, X.-M. Ren, C.-Y. Duan, Y. Xu, S. Gao, X.-Z. You, Chem. Eur. J. 9 (2003) 5673–5685.
[6] M. Kurmoo, C.J. Kepert, New J. Chem. (1998) 1515–1524;
S.R. Batten, K.S. Murray, Coord. Chem. Rev. 246 (2003) 103–130.
[7] T. Lancaster, S.J. Blundell, F.L. Pratt, M. Kurmoo, Physica B 326 (2003) 522–526.
[8] M. Ohba, H. Okawa, Coord. Chem. Rev. 198 (2000) 313–328;
C.N.R. Rao, S. Natarajan, R. Vaidhyanathan, Angew. Chem. Int. Ed. 43 (2004) 1466–1496.
[9] Z.-M. Wang, B. Zhao, H. Fujiwara, H. Kobayashi, M. Kurmoo, Chem. Commun. (2004) 416–417;
Z.-M. Wang, B. Zhang, T. Otsuka, K. Inoue, H. Kobayashi, M. Kurmoo, Dalton Trans. (2004) 2209–2215;
Z.-M. Wang, B. Zhang, M. Kurmoo, M.A. Green, H. Fujiwara, T. Otsuka, H. Kobayashi, Inorg. Chem. 44 (2005) 1230–1237;
Z.-M. Wang, Y. Zhang, M. Kurmoo, T. Liu, S. Vilminot, B. Zhao, S. Gao, Aust. J. Chem. 59 (2006) 617–621;
Z.-M. Wang, B. Zhang, K. Inoue, H. Fujiwara, T. Otsuka, H. Kobayashi, M. Kurmoo, Inorg. Chem. 46 (2007) 437–445;
B. Zhang, Z.-M. Wang, M. Kurmoo, S. Gao, K. Inoue, H. Kobayashi, Adv. Funct. Mater. 17 (2007) 577–584;
Z.-M. Wang, B. Zhang, Y.-J. Zhang, M. Kurmoo, T. Liu, S. Gao, H. Kobayashi, Polyhedron 26 (2007) 2207–2215;
Z.-M. Wang, Y. Zhang, T. Liu, M. Kurmoo, S. Gao, Adv. Funct. Mater. 17 (2007) 1523–1536;
Z.-M. Wang, X. Zhang, S.R. Batten, M. Kurmoo, S. Gao, Inorg. Chem. 46 (2007) 8439–8441.
[10] Y. Yoshida, K. Inoue, N. Kyritsakas, M. Kurmoo, Inorg. Chim. Acta 362 (2009) 1428–1434.
[11] B. Kratochvil, J. Podlahova, S. Habibpur, V. Petricek, K. Maly, Acta Crystallogr B 38 (1982) 2436–2438.
[12] R. Chmelikova, J. Loub, V. Petricek, Acta Crystallogr. C 42 (1986) 1281–1283.
[13] R. Ouarsal, A.A. Tahiri, B.E. Bali, M. Lachkara, W.T.A. Harrison, Acta Crystallogr. E 58 (2002) i23–i25.
[14] W. Liu, H.H. Chen, X.X. Yang, J.T. Zhao, Eur. J. Inorg. Chem. (2005) 946–951.
[15] C.Y. Ortiz-Avila, P.J. Squattrito, M. Shieh, A. Clearfield, Inorg. Chem. 28 (1989) 2608–2615.
[16] R. Ouarsal, A.A. Tahiri, M. Lachkar, M. Dusek, K. Fejfarova, B.E. Bali, Acta Crystallogr. E 59 (2003) i33–i35.
[17] G.M. Sheldrick, SHELXS97 and SHELXL97, University of Gottingen, Germany.
[18] H.A. Maouel, V. Alonzo, T. Roisnel, H. Rebbah, E.Le Fur, Acta Crystallogr. C 65 (2009) i36–i38.
[19] M.D. Marcos, P. Amoros, A. Beltran-Porter, R. Martinez-Manez, J.P. Attfield, Chem. Mater. **5** (1993) 121–128;
W.T.A. Harrison, Solid State Sci. 5 (2003) 297–302;
M.D. Marcos, P. Amoros, A.L. Bail, J. Solid State Chem. 107 (1993) 250–257.
[20] F. Hanic, Z. Zak, J. Solid State Chem. **10** (1974) l2–l9;
M. Ferid, K. Horchani, J. Amami, Mater. Res. Bull. 39 (2004) 1949–1955;
F. Sanz, C. Parada, J.M. Rojo, C. Ruiz-Valero, Chem. Mater. 11 (1999) 2673–2679;
B.B. Kratochvil, J. Podlahova, S. Habibpur, Acta Crystallogr. B 38 (1982) 2436–2438.
[21] U.C. Chunga, J.L. Mesa, J.L. Pizarro, V. Juberac, L. Lezamab, M.I. Arriortua, T. Rojo, J. Solid State Chem. 178 (2005) 2913–2921;
B. Manoun, B. El Bali, S.K. Saxena, R.P. Gulve, J. Mol. Struct. 794 (2006) 334–340.
[22] M. Tsuboi, J. Am. Chem. Soc. 79 (1957) 1351–1354.
[23] R.I. Bickley, H.G.M. Edwards, A. Knowles, J.K.F. Tait, R.E. Gustar, D. Mihara, S.J. Rose, Spectrochimica Acta Part A: Molecular Spectroscopy **50** (1994) 1277–1285.
[24] J. Baran, Z. Czapla, M.K. Drozd, M.M. Ilczyszyn, M. Marchewka, H. Ratajczak, J. Mol. Struct. 403 (1997) 17–37.